

Investigating the use of HSE Hybrid Functionals to Improve Electron Transport Calculations in Si, Ge, Diamond, and SiC

Dallin Nielsen¹, Maarten Van de Put², Massimo Fischetti³
Dept. of Materials Science and Engineering, The University of Texas at Dallas
Dallas, USA

don170000@utdallas.edu¹, Maarten.VandePut@utdallas.edu², max.fischetti@utdallas.edu³

Abstract— In this work, we employ density functional theory with HSE hybrid functionals (HFs) to calculate the electronic band structure of Si, Ge, diamond, and SiC in an attempt to improve upon electron-phonon scattering rates calculated with conventional PBE exchange-correlation functionals. To check for possible improvements, the band structure of each material calculated with the PBE functional is compared to that obtained with HSE HFs. The first point of comparison is the effective electron mass at the conduction band (CB) minimum. These values are calculated and compared to experimental data. In addition, the joint density of states (JDOS) is calculated for each material. Peaks and shoulders in the JDOS plot (representing transition energies at symmetry points in the band structure) are compared to the values obtained experimentally. The results show that there is no consistent improvement in the calculated effective masses or symmetry point locations from PBE to HSE, suggesting a ‘compression’ of the CB that may affect the calculated electron-phonon scattering rates.

Keywords—Electron transport, DFT, HSE, hybrid functionals, scattering rates.

I. INTRODUCTION

The theoretical investigation of phonon-limited electron transport in semiconductors has been key to the development of virtually all modern electronic devices. A vital part of this study is the accurate calculation of the electron-phonon scattering rates. Currently, one of the most prevalent methods to perform this calculation is density functional theory (DFT). It is used to produce the electronic band structure (band structure), phonon dispersion, and subsequently, electron-phonon matrix elements of a given material, which can be used in Fermi’s Golden Rule to obtain scattering rates. Given the built-in assumptions of DFT, and the fact that it is a “ground state” theory, the success it has thus far achieved in transport calculations is truly remarkable. Still, while DFT has become an extremely useful computational tool, problems remain [1,2].

Indeed, even in Si things are “iffy”, as recently published works show contradictions in electron scattering and energy loss rates [3,4]. One of the major issues associated with DFT is a “compression” of the conduction bands (CBs). We believe this compression, unfortunately, affects the scattering rates for two reasons: Firstly, the electron-phonon matrix elements are shifted in energy due to this compression and, secondly, the density of final states available to scattering carriers is increased, as a result of band flattening. Much of the trouble in DFT arises from the approximation of the exchange-correlation functional in the

Kohn-Sham equations [5]. A common exchange-correlation functional that is widely used is the generalized gradient approximation (GGA) PBE functional [6]. Over the years, corrections to the exchange-correlation functional have been proposed to generate more accurate results. One of these is HSE hybrid functionals (HFs) [7], which mix a fraction of exact exchange from Hartree-Fock theory with the rest of the exchange-correlation energy from PBE. HSE HFs have been widely used to correct the primary band gap [8], and claims have even been made that they yield more accurate effective electron masses at the CB minimum [9]. In this paper, we investigate the use of HSE HFs to improve the calculated electronic band structure of Si, Ge, diamond, and SiC over the band structure calculated with conventional PBE functionals in attempts to solve the CB compression issue.

II. METHODOLOGY

To begin, we calculated the band structures for the abovementioned materials, using the DFT package Quantum ESPRESSO (QE). As described above, the band structure was calculated for each material using both the conventional PBE and HSE methods. Going forward, we will refer to them as PBE and HSE, respectively. For both cases, fully relativistic SG15 Optimized Norm-Conserving Vanderbilt (ONCV) pseudopotentials were used. We included spin-orbit coupling in the calculations. In the case of HSE, we employed a trial-and-error process to determine the respective fractions of exact exchange for each material (Si: 0.07, Ge: 0.08, diamond: 0.11, SiC: 0.1) that yield a value for the band gap closest to the available experimental data.

To demonstrate the effects of the CB compression on electron-phonon scattering rates, we further used density functional perturbation theory (DFPT) in QE to generate the phonon dispersions for each material. These dispersions, with the electronic band structure, were fed into the code Electron-Phonon Wannier (EPW) to obtain electron-phonon matrix elements [10]. With these matrix elements, we then used Fermi’s Golden Rule,

$$\frac{1}{\tau_i^{(\eta)}} = \frac{2\pi}{\hbar} \sum_{jq} |M_{ij}^{(q,\eta)}|^2 \delta[E_i - E_j \pm \hbar\omega_q^{(\eta)}], \quad (1)$$

to calculate scattering rates, $1/\tau_i^{(\eta)}$, for an electron in the initial state i with phonons of mode η . The quantity $M_{ij}^{(q,\eta)}$ is the matrix element for scattering from state i to state j by a phonon

\mathbf{q} of mode η , E_i and E_j are the initial and final energies, respectively, and $\hbar\omega_{\mathbf{q}}^{(\eta)}$ is the energy associated with the phonon \mathbf{q} of mode η . The determination of the density of final states was carried out using the tetrahedron method, a common numerical technique used for Brillouin zone (BZ) integration [11].

To observe the differences between the PBE and HSE band structures, we selected two points of comparison. These include first, the effective electron masses at the CB minimum and second, the energies associated with direct transitions across the energy gap at certain symmetry points in the BZ. Indeed, experimental data on the electron effective mass are widely available, and this quantity is a good indicator of how well the transport characteristics of a material will match experiment. Second, experimental information on the energies of direct transitions at symmetry points is also widely available from the dielectric function, electro-reflectance, and optical absorption spectra, for example. This information can help us to quantify and visualize the CB compression.

To determine the effective masses, we fit polynomials to the band structure data of each material at the CB minimum and extracted the longitudinal and transverse effective masses.

For the energies at symmetry points, we calculated the joint density of states (JDOS), again with the tetrahedron method. The JDOS is the density of states associated with direct transitions from the highest valence band (VB) into the CBs, and it is defined as:

$$JDOS(E) = \frac{2}{\Omega_c} \sum_{mk} \delta[E - (E_m(\mathbf{k}) - E_n(\mathbf{k}))], \quad (2)$$

where Ω_c is the unit cell volume, m indicates the CB index, and n is the index of the highest VB. A large JDOS indicates a high likelihood of a given transition. Peaks and shoulders in the JDOS vs. energy plot represent transitions at symmetry points. Therefore, the JDOS plot can be compared to measured energies of transitions at symmetry points to check for the accuracy of the band structure results. For this comparison, we shifted the CB energy so that the energy gap was corrected, since conventional DFT calculations underestimate this value.

III. RESULTS AND DISCUSSION

To first observe the CB compression, we plotted the band structure of Si in Fig. 1. The compression can be seen by looking at the energy distances between the CB minimum and L_{c1} and L_{c2} . Experimentally, these distances have been found to be 1.05 eV and 3.13 eV, respectively [12]. In the calculated band structure, however, these distances are shrunk to 0.83 eV and 2.73 eV: reductions of 21% and 13%, respectively. The effect of this CB compression on the electron-phonon scattering rates is a compression of the rates to lower energies and a general magnification. This can be seen by comparing our PBE results in Fig. 2 (b) to scattering rates published by other groups in Fig. 2 (a). It is clear that our results agree with the PBE rates in Fig. 2 (a), but they are as much as ~45% larger than the others, which were calculated using empirical pseudopotentials and Harris potentials and have yielded transport-related results that compare successfully to experimental results (see Ref. [3]).

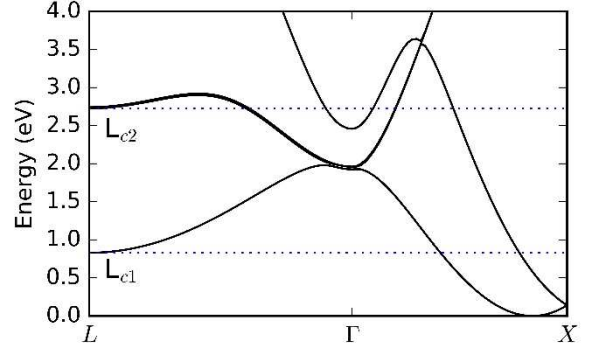


Fig. 1. The CBs of Si, calculated using DFT with PBE plotted with respect to the bottom of the CBs. L_{c1} and L_{c2} indicate the L points of the first and second CBs, respectively.

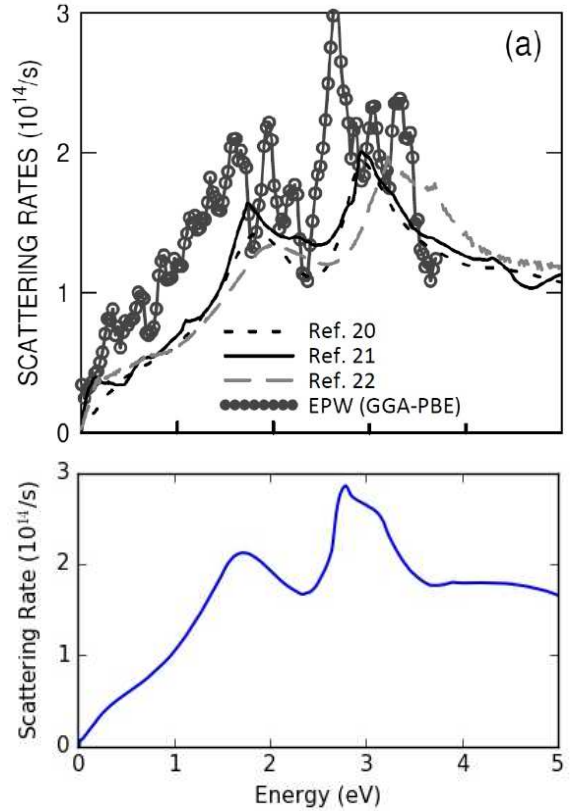


Fig. 2. (a) Electron-phonon scattering rates of Si (averaged over equi-energy shells), calculated using PBE functionals in EPW [3] compared to the rates published in [20,21,22] (adapted from [3]). (b) Rates that we have obtained using PBE in EPW.

Having now established the existence of CB compression in the PBE case, we now look at the results from the HSE calculations. Table 1 shows both the energy gap and effective mass results for both PBE and HSE. It is clear that HSE HF's significantly improve the energy gap, as expected. For the effective masses, however, we see no consistent improvement.

Looking now at the symmetry points, Fig. 3 shows the JDOS for each material. The experimentally measured direct transitions at the labeled symmetry points are shown by dashed lines. These same transitions, as calculated by PBE and HSE are

Table 1. Calculated and experimental energy gaps and effective masses. Effective masses are measured in units of the free electron mass (m_0). Here, m_t and m_l are the transverse and longitudinal masses, respectively.

Material	Gap (eV)			Effective mass					
	Exp.	PBE	HSE	Experiment		PBE		HSE	
				m_t/m_0	m_l/m_0	m_t/m_0	m_l/m_0	m_t/m_0	m_l/m_0
Si	1.12	0.5861	1.0898	0.19 [13]	0.98 [13]	0.2078	0.9736	0.2064	0.9564
Ge	0.66 [14]	-0.069	0.6341	0.082 [15]	1.59 [15]	0.213	1.7386	0.1802	1.6916
Diamond	5.48 [16]	4.194	5.5243	0.36 [17]	1.4 [17]	0.3169	1.6563	0.2878	1.5933
SiC	2.39 [18]	1.3865	2.3638	0.25 [19]	0.67 [19]	0.2421	0.6773	0.2427	0.6562

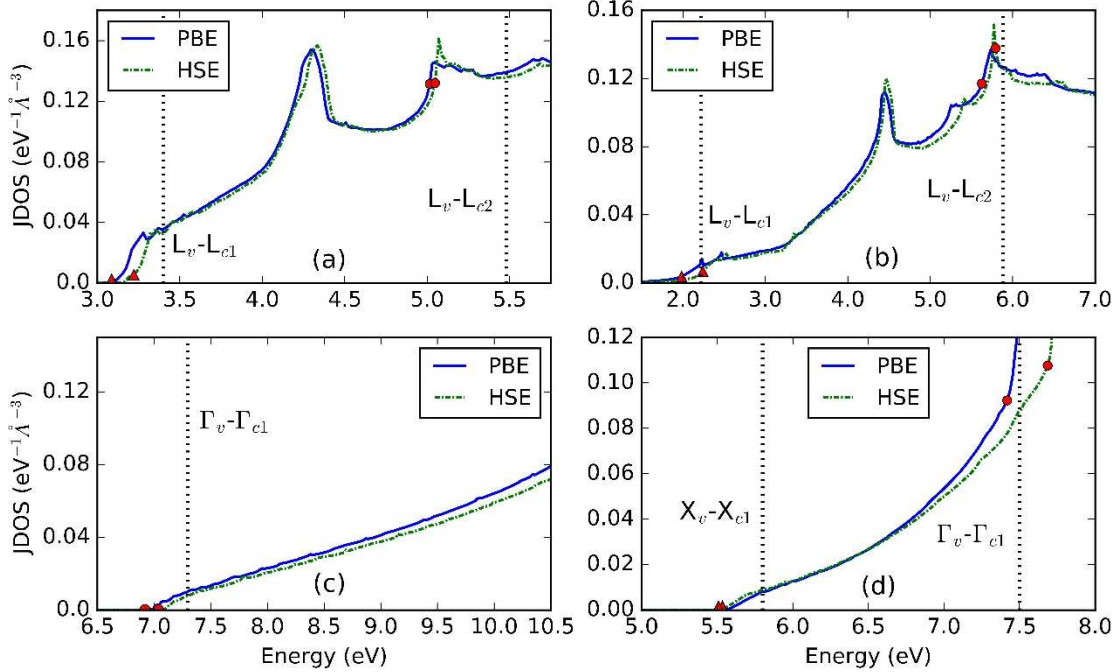


Fig. 3. The JDOS of (a) Si, (b) Ge, (c) diamond, and (d) SiC adjusted to the correct energy gaps. Experimentally measured direct transitions are indicated by dashed lines. Their labels indicate which symmetry point transitions they represent. Subscripts ‘v’ and ‘c’ refer to VBs and CBs, respectively, and the numbers refer to the CB number. Small shapes (triangle and dots) are used to indicate where these transitions occur on the PBE and HSE plots. For most of the plots, triangles refer to the lower-energy transition, while dots refer to the higher-energy transition. For diamond, only one transition is indicated with dots [12,23,24].

indicated by triangles (lower-energy transitions) or dots (higher-energy transitions). In all materials the transitions from PBE calculations occur at lower energies than the experimental data. This is yet another indication of CB compression. With the application of HSE, some decompression can be observed in all cases. The extent of decompression is clearly material-dependent. In addition, we see variable decompression over the energy range for a given material. For example, in Si, there is decent decompression at the L_v-L_{c1} transition, but scant decompression at the L_v-L_{c2} transition. Overall, again, we observe no consistent improvement in the results with the application of HSE.

With these rather disappointing outcomes from the effective mass and JDOS calculations, one would logically surmise that the HSE electron-phonon scattering rates would show little to no improvement over PBE rates. And, indeed this is what we observe in performing the calculation. The results are depicted in Fig. 4. In the HSE case, we used PBE electron-phonon matrix elements mixed with HSE density of final states in Fermi’s

Golden Rule. This mixture was necessary because QE currently does not allow for the calculation of electron-phonon matrix elements with HFs. Still, this calculation gives a good first approximation of the HSE rates. We recall now, from Fig. 2, that the two major effects of the CB compression on the scattering rates were a shift to lower energies and an overall increase in magnitude. It is evident from the plots that the HSE rates exhibit some shift toward higher energies, especially in diamond and SiC. This, of course, is related to the decompression of the CBs observed in Fig. 3. The shift, however, is small and, in some cases, nonexistent. Additionally, there is very little reduction in magnitude seen, and it only seems to occur in spots. Given that the Si rates in Fig. 2 were as much as 45% larger than the experimentally verified rates, there would need to be a much more significant reduction. Generally, therefore, there appears to be no substantial improvement in the rates with the use of HSE.

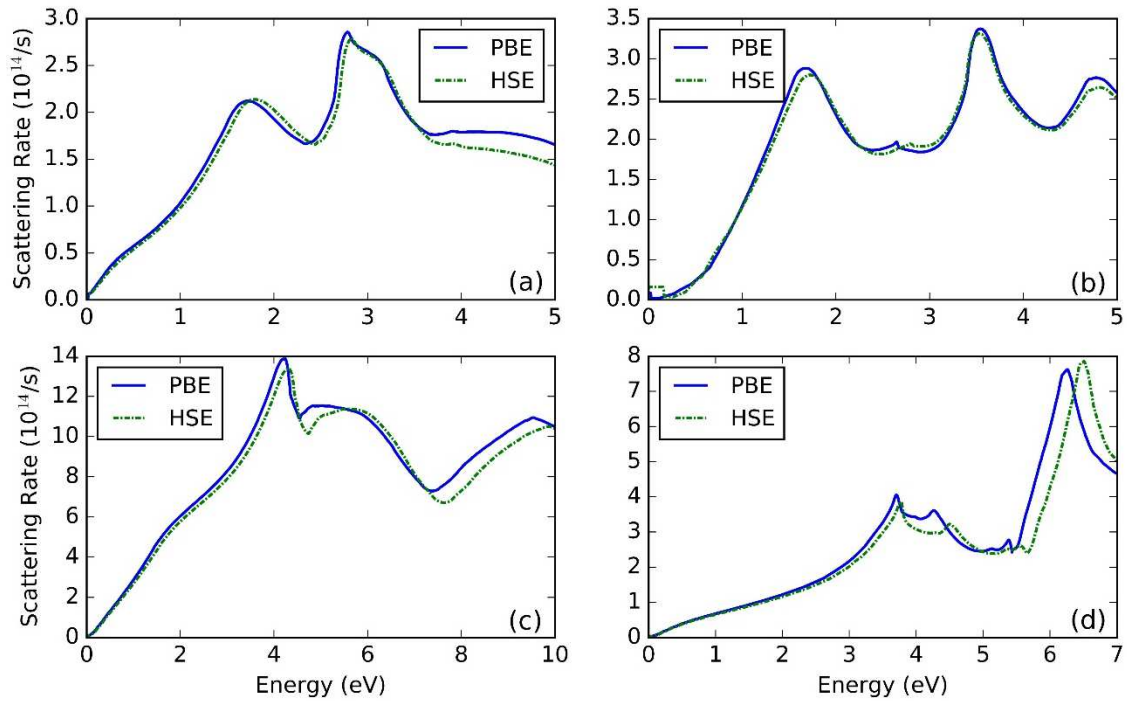


Fig. 4. The electron-phonon scattering rates of (a) Si, (b) Ge, (c) diamond, and (d) SiC as calculated using PBE and HSE functionals.

IV. CONCLUSIONS

We have presented an investigation of the use of HSE HF's for the improvement of the DFT band structure calculation to obtain more accurate electron-phonon scattering rates. We have shown the results of effective mass, JDOS, and scattering rate calculations for both the conventional PBE and HSE HF cases. In both the effective mass and JDOS results, we observed no consistent improvement in the major problem associated with DFT of CB compression. While some decompression is seen, its extent is variable, even for the same material. Additionally, as seen in SiC, the decompression can go too far, pushing a given symmetry point to energies that are larger than experiments suggest. And, in finally looking at the scattering rate results, we demonstrated that the HSE rates were not substantially better than those from PBE. And, given that HSE is far more computationally expensive than PBE, any minor improvements may not be worth the cost. We therefore conclude that HSE HF's do not produce a necessarily more accurate band structure for transport calculations.

REFERENCES

- [1] G. Gaddemane, S. Gopalan, M. L. Van de Put, and M. V. Fischetti, *J Comput. Electron.* 20, 49-59 (2021).
- [2] G. Gaddemane, W.G. Vandenberghe, M. L. Van de Put, S. Chen, S. Tiwari, E. Chen, and M. V. Fischetti, *Phys. Rev. B* 98, 115416 (2018).
- [3] M. V. Fischetti, P. D. Yoder, M. M. Khatami, G. Gaddemane, and M. L. Van de Put, *Appl. Phys. Lett.* 114, 222104 (2019).
- [4] S. Ponc e, E. R. Margine, and F. Giustino, *Phys. Rev. B* 97, 121201 (R) (2018).
- [5] W. Kohn, L.J. Sham, *Phys. Rev.* 140, A1133 (1965).
- [6] Perdew, John P.; Kieron Burke; Matthias Ernzerhof (1996-10-28). "Generalized Gradient Approximation Made Simple". *Physical Review Letters*. 77 (18): 3865–3868
- [7] Cite Jochen Heyd; Gustavo E. Scuseria; Matthias Ernzerhof (2003). "Hybrid functionals based on a screened Coulomb potential". *J. Chem. Phys.* 118 (18): 8207
- [8] Y. Matsushita, K. Nakamura, A. Oshiyama, *Phys. Rev. B* 84, 075205 (2011).
- [9] H. Peelaers and C. G. Van de Walle, *Phys. Status Solidi B* 252, No. 4, 828–832 (2015).
- [10] S. Ponc e, E.R. Margine, C. Verdi, F. Giustino, *Computer Physics Communications*, Volume 209 (2016).
- [11] P. E. Bl ochl, O. Jepsen, and O. K. Andersen, *Phys. Rev. B* 49, 16223 (1994).
- [12] J. R. Chelikowsky, M. L. Cohen, *Phys. Rev. B* 30, 4828 (1984).
- [13] R. N. Dexter, B. Lax, A. F. Kip, and G. Dresselhaus, *Phys. Rev.* 96, 222 (1954).
- [14] O. Madelung, U. R ossler, and M. Schulz (Eds.), *Numerical Data and Functional Relationships in Science and Technology, Landolt–B ornstein, New Series, Group III, vol. 17a, and 22a, Springer, 2006.*
- [15] C. Kittel: "Introduction to Solid State Physics," 8th ed., p. 202, John Wiley & Sons, Inc. New York. 2005.
- [16] H. Lofas, A. Grigoriev, J. Isberg, and R. Ahuja, *AIP Advances* 1, 032139 (2011).
- [17] F. Nava, C. Canali, C. Jacoboni, L. Reggiani, and S. F. Kozlov, *Solid State Communications* 33, 475 (1980).
- [18] *Physics of Group IV Elements and III-V Compounds, Landolt–Bornstein, New Series, Group III, edited by O. Madelung, M. Schulz, and M. Weiss (Springer, Berlin, 1982), Vol. 17, Pt. a*
- [19] J. Kono, S. Takeyama, H. Yokoi, N. Miura, M. Yamanaka, M. Shinohara, and K. Ikoma, *Phys. Rev. B* 48, 10909 (1993).
- [20] M.V. Fischetti and J.M. Hignman, Theory and calculation of the deformation potential electron-phonon scattering rates in semiconductors, in *Monte Carlo Device Simulation: Full Band and Beyond*, ed. by K. Hess (Kluwer Academic, Norwell, 1991), pp. 123–160.
- [21] P.D. Yoder, J.M. Hignman, J.D. Bude, and K. Hess. *Semicond. Sci. Technol.* 7, B357–B359 (1992).
- [22] M.V. Fischetti and S.E. Laux. *Phys. Rev. B* 38, 9721–9745 (1988).
- [23] R. A. Roberts and W. C. Walker, *Phys. Rev.* 161, 730 (1967).

[24] W. R. Lambrecht, S. Limpijumnong, S. N. Rashkeev, and B. Segall, Phys. Status Solidi B 202, 5 (1997).